SINGULAR LANGMUIR–HINSHELWOOD REACTION-DIFFUSION PROBLEMS: STRONGLY NONISOTHERMAL CONDITIONS*

JOSE M. VEGA†

Abstract. The steady state reaction-diffusion problem for a permeable catalytic particle is considered, when the reaction rate is of the Langmuir–Hinshelwood type and the activation energy is large. It is shown that there are multiple solutions for the Damköhler number belonging to a certain interval. An arbitrarily large number of solutions appear for symmetric particles: (a) in two dimensions if the adsorption effects are sufficiently important and the reaction order is negative, and (b) in three dimensions. An asymptotic analysis provides approximate analytical expressions for the response curves and for the multiplicity bounds.

1. Introduction. Let us consider a catalytic decomposition of the type $A \rightarrow$ Products in a permeable particle. For the chemical reaction to be catalyzed by the solid, the reactant A must be adsorbed at the walls of the pores of the particle. This adsorption-reaction process may be modelled by a kinetic law of the Langmuir–Hinshelwood type. The governing equations are obtained from the principle of continuity applied to the reactant and to the enthalpy. After suitable nondimensionalization, they may be written in the form (see Aris [1])

$$\frac{d^2c}{dx^2}+\frac{j}{x}\frac{dc}{dx}=-\frac{1}{\bar{\beta}}\left(\frac{d^2t}{dx^2}+\frac{j}{x}\frac{dt}{dx}\right)=\Phi^2\frac{c^n\exp\left(\bar{\gamma}(t-1)/t\right)}{\{1+K_ac\exp\left(-\bar{\gamma}_a(t-1)/t\right)\}^p} \tag{1.1}$$

where $c>0$ is the concentration of A, $t>0$ is the temperature and x is the distance to the center of the particle. The particle is assumed to be an infinite slab, cylinder or a sphere ($j=0$, 1 or 2 resp.) and only solutions having the same symmetry as the particle are considered. In addition to the symmetry condition at the center,

$$\frac{dc}{dx}=\frac{dt}{dx}=0 \quad \text{at } x=0, \tag{1.2}$$

Robin type boundary conditions are imposed at the surface

$$\sigma(1-c)=\frac{dc}{dx}, \qquad \nu(1-t)=\frac{dt}{dx} \quad \text{at } x=1. \tag{1.3}$$

The parameters $\bar{\beta}$, $\bar{\gamma}$, $\bar{\gamma}_a$, K_a, ν and σ are positive, while the reaction orders n and p are assumed to be $n, p \geqq 1$.

The observable reaction rate per unit volume, $\bar{\psi}$, which is given by

$$\bar{\psi}=(j+1)\left(\frac{dc}{dx}\right)_{x=1},$$

is of physical importance because it gives the intensity of the particle as a sink of reactant. The curves $\bar{\psi}-\Phi$ (for fixed values of the remaining nondimensional parameters of the problem) are called response curves.

System (1.1)–(1.3) has received considerable attention in the chemical engineering literature (see [1], [4], [5] and references given there). It adequately represents CO oxidation over platinum catalysts, which is the main reaction in automotive pollution abatement efforts. There is experimental evidence that the oxidation of several

* Received by the editors November 2, 1982.

† Escuela Tecnica Superior de Ingenieros Aeronáuticos, Universidad Politécnica de Madrid, Madrid–3, Spain.

hydrocarbons, such as ethylene and propylene, over noble metal catalysts may be represented by similar models.

Numerical computations of (1.1)–(1.3) were made by Carberry and Hutchings [2] and by Schneider et al. [3] for $n = p = 1$, and by Smith et al. [4] for $n = 1$ and $p = 2$. Their results suggest that (1.1)–(1.3) has multiple solutions for Φ in a certain interval if $\bar{\gamma} \cdot \bar{\beta}$ exceeds a certain critical value or if K_a is sufficiently large and $n < p$.

Pereira and Varma [5] gave lower and upper bounds of the multiplicity interval; the former appeared to be too conservative for large values of K_a.

An asymptotic analysis of the limit $\bar{\gamma} \cdot \bar{\beta} \to \infty$ for Arrhenius kinetics ($p = 0$) was made independently by Urrutia and Liñán [6] and Kapila et al. [7], [8]. For the Dirichlet problem ($\sigma = \nu = \infty$), they showed that the response curve is S-shaped in slabs and cylinders, while for spheres it has a spiral shape (as in sketch 3 in Fig. 1b), with an arbitrarily large number of solutions for certain values of Φ and sufficiently large values of $\bar{\gamma} \cdot \bar{\beta}$.

The limit $\bar{\gamma} \cdot \bar{\beta} \to 0$ and $K_a \to \infty$ was considered by Vega and Liñán [9]. For $\sigma = \nu = \infty$ and the slab geometry, it was shown that $\bar{\psi}$ depends monotonously on Φ if $n \geqq p$ while the response curve is S-shaped if $n < p$; for cylinders (spheres) Φ depends monotonously on ψ if $n \geqq p$ ($n \geqq p + (11 - \sqrt{2})/7$) and the response curve has a spiral shape otherwise.

In this paper, (1.1)–(1.3) will be analyzed in the limit

$$\bar{\gamma} \cdot \bar{\beta} \to \infty, \qquad \bar{\beta} = O(1). \tag{1.4}$$

Additional assumptions about the order of magnitude of the parameters are

$$\sigma, \frac{\sigma}{\nu} \to \infty, \qquad \frac{\bar{\beta}}{\nu}, K_a^{-1} = O(1), \tag{1.5}$$

as taken from their usual values in practice.

In § 2, (1.1)–(1.3) is reduced to a simpler problem with boundary conditions of the Dirichlet type, which is analyzed in detail in §§ 3–6. The results do match with those of references [6]–[9], namely, the response curve is S-shaped for $j = 0$, $j = 1$ and $n \geqq p$ or $j = 1$, $n < p$ and K_a sufficiently small, while it has a spiral shape if $j = 1$, $n < p$ and K_a is sufficiently large or if $j = 2$. Finally, the results of §§ 3–6 are used, in § 7, to analyze (1.1)–(1.3).

2. The Dirichlet problem. When the concentration and temperature are nondimensionalized with their values at the surface of the particle, the boundary conditions (1.3) become of the Dirichlet type. To attain this reduction, the following variables and parameters are used:

$$y = \frac{c}{c_s}, \qquad T = \frac{t}{t_s}, \qquad \gamma = \frac{\bar{\gamma}}{t_s}, \qquad \gamma_a = \frac{\bar{\gamma}_a}{t_s}, \qquad \beta = \frac{\bar{\beta} c_s}{t_s},$$
$$k = \frac{\exp(\bar{\gamma}_a (t_s - 1)/t_s)}{K_a c_s}, \qquad \phi^2 = \Phi^2 c_s^{n-1} \frac{k^p \exp(\bar{\gamma}(t_s - 1)/t_s)}{(k+1)^p} \tag{2.1}$$

where $c_s = c(1)$ and $t_s = t(1)$. (1.1)–(1.3) is then written in the form

$$\frac{d^2 y}{dx^2} + \frac{j}{x}\frac{dy}{dx} = -\frac{1}{\beta}\left(\frac{d^2 T}{dx^2} + \frac{j}{x}\frac{dT}{dx}\right) = \phi^2 \frac{(k+1)^p y^n \exp(\gamma(T-1)/T)}{\{k + y \exp(-\gamma_a (T-1)/T)\}^p}, \tag{2.2}$$

$$\frac{dy}{dx} = \frac{dT}{dx} = 0 \quad \text{at } x = 0, \qquad y = T = 1 \quad \text{at } x = 1, \tag{2.3}$$

where the boundary condition at $x = 1$ is a consequence of the definition of y and T. The observable reaction rate is now defined as

$$\psi = (j+1)\left(\frac{dy}{dx}\right)_{x=1} = \frac{\bar{\psi}}{c_s}. \tag{2.4}$$

The boundary conditions (1.3) and the so-called Prater relation,

$$T = 1 + \beta(1-y), \tag{2.5}$$

which is easily obtained from the first equation of (2.2), lead to the following expressions for c_s and t_s:

$$c_s = \left(1 + \frac{\psi}{(j+1)\sigma}\right)^{-1}, \qquad t_s = 1 + \frac{\bar{\beta}\psi}{(j+1)\nu}\left(1 + \frac{\psi}{(j+1)\sigma}\right)^{-1}. \tag{2.6}$$

As we shall see in detail in § 7, the response curves $\bar{\psi} - \Phi$ of the Robin problem (1.1)–(1.3) may be obtained, via (2.1) and (2.4)–(2.6), from the curves $\psi - \phi$ of the Dirichlet problem (2.2)–(2.3), which will be analyzed first, in the following sections.

The relation (2.5) allows us to write (2.2)–(2.3) in terms only of the concentration y:

$$\frac{d^2y}{dx^2} + \frac{j}{x}\frac{dy}{dx} = \phi^2(k+1)^p\left(k + y\exp\left(-\frac{\gamma_a\beta(1-y)}{1+\beta(1-y)}\right)\right)^{-p} \cdot y^n \exp\left(\frac{\gamma\beta(1-y)}{1+\beta(1-y)}\right), \tag{2.7}$$

$$\left(\frac{dy}{dx}\right) = 0 \quad \text{at } x = 0, \qquad y = 1 \quad \text{at } x = 1. \tag{2.8}$$

If $\psi = O(1)$, then $c_s^{-1} \sim t_s \sim 1$ (see (1.4), (1.5), (2.6)) and

$$\gamma\beta = \bar{\gamma}\bar{\beta}\frac{c_s}{t_s^2} \gg 1,$$

as will be assumed in §§ 3–6. This may be no longer true for ψ sufficiently large. But for $\psi \gg 1$, $\beta \ll 1$ and $\gamma\beta = O(1)$, the response curve is given, in first approximation, by

$$\phi^2 = \frac{1}{2}(k+1)^{-p}\left(\frac{(1+\beta)^2}{\gamma\beta}\right)^{p-n-1}\left(\frac{\psi}{(j+1)}\right)^2 \frac{\exp\left(-(\gamma + p\gamma_a)\beta/(1+\beta)\right)}{f_{np}(\mu, \gamma\beta/(1+\beta)^2)} \tag{2.9}$$

where

$$f_{np}(\mu, z) = \int_0^z \frac{u^n e^{-u}}{(\mu+u)^p}\,du, \tag{2.10}$$

as may be obtained by an asymptotic analysis of (2.7)–(2.8) (see Murray [10]).

Observe that $\gamma_a\beta < \bar{\gamma}_a\bar{\beta}$ is a quantity of order $O(1)$ for $\psi \in [0, \infty[$.

3. The ignition regime. This regime describes the branch OA of the response curve in Fig. 1, and corresponds to the distinghished limit $\phi^2 \sim \psi \sim (\gamma\beta)^{-1}$. When the expansions

$$\phi^2 = (\gamma\beta)^{-1}\Lambda_0(1 + (\gamma\beta)^{-1}\delta_1 + \cdots), \tag{3.1}$$

$$y = 1 - (\gamma\beta)^{-1}g_0 - (\gamma\beta)^{-2}((2\beta - a)(1+g_0) + \beta g_0^2 - \delta_1 + \beta g_1) + \cdots, \tag{3.2}$$

$$a = p\frac{1+\gamma_a\beta}{k+1} - n$$

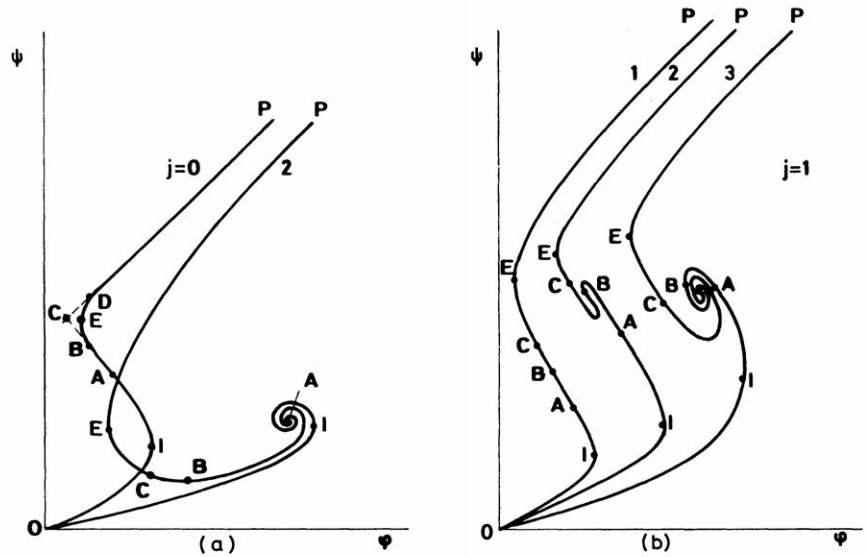

FIG. 1. *Sketch of the response curves for the Dirichlet problem* (2.7)–(2.8). (a) *Slabs and spheres*, (b) *cylinders for* $n > p$ *(curve* 1), $n < p$ *and* $\mu \to \infty$ *(curve* 2) *and* $n < p$ *and* $\mu \to 0$ *(curve* 3).

are inserted into (2.7)–(2.8), g_0 and g_1 are found to be given by

$$g_0'' + jx^{-1}g_0' = -\Lambda_0 \exp(g_0), \qquad g_0'(0) = g_0(1) = 0, \tag{3.3}$$

$$\begin{aligned} &g_1'' + jx^{-1}g_1' = -\Lambda_0 \exp(g_0)g_1 - 2g_0'^2, \\ &g_1'(0) = 0, \qquad \beta g_1(1) + 2\beta - a = \delta_1. \end{aligned} \tag{3.4}$$

The problem (3.3) has been considered in a number of works, beginning with Endem [11]; see [1] and [12] for further references. It is well known, in particular, that (3.3) may be reduced to a canonical initial value problem by use of the appropriate variables. This is a consequence of the invariance of the differential equation and the boundary condition at $x = 0$ under the continuous group of transformations

$$\Lambda_0 \to \alpha_1^2 \Lambda_0, \quad g_0 \to g_0 + 2\alpha_2, \quad x \to \alpha_1^{-1} e^{-\alpha_2} x. \tag{3.5}$$

In the new variables,

$$\omega_0 = -(j+1)xg_0', \quad \theta_0 = \Lambda_0 x^2 \exp g_0, \quad s = g_0(0) - g_0, \tag{3.6}$$

which are chosen to be invariant under the group and to take meaningful values at $x = 1$, $g_0 = 0$ (see (3.9) below), (3.3) is written as

$$\frac{d\omega_0}{ds} = 1 - j^2 + (1+j)^2 \frac{\theta_0}{\omega_0}, \qquad \frac{d\theta_0}{ds} = 2(j+1)\frac{\theta_0}{\omega_0} - \theta_0, \tag{3.7}$$

$$\lim \frac{\omega_0}{s} = \lim \frac{\theta_0}{s} = 2(j+1) \quad \text{as } s \to 0^+, \tag{3.8}$$

$$\omega_0 = -(j+1)g_0'(1), \quad \theta_0 = \Lambda_0 \quad \text{at } s = g_0(0). \tag{3.9}$$

For $j=0$ and 1, the initial value problem (3.7)–(3.8) has the solutions

$$j=0: \quad \frac{\omega_0}{\sqrt{e^s-1}}=\sqrt{\frac{\theta_0}{2}}=e^{-s/2}\ \text{arg Ch}\,(e^{s/2}),$$

$$j=1: \quad \omega_0=e^{s/2}\theta_0=8(1-e^{-s/2}),$$

while for $j=2$ no closed-form solution of it is known (see Steggerda [13] for precise numerical results). It is easily seen that, for $j=2$, the solution of (3.7)–(3.8) spirals around the critical point $(\omega_0, \theta_0)=(6, 2)$ of the phase plane as $s\to\infty$. A graph of the curve $\omega_0-\theta_0$ is given in Fig. 2.

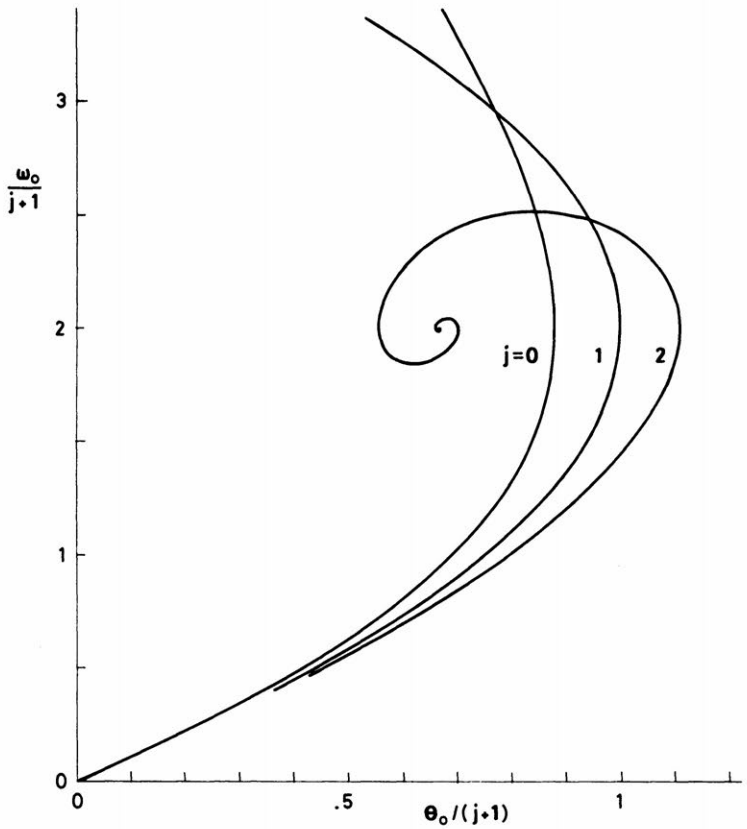

FIG. 2. *The curves* $\omega_0-\theta_0$ *satisfying* (3.7)–(3.8).

The linear problem (3.4) can also be reduced to a canonical initial value problem because, again, the differential equation and the boundary condition at $x=0$ are invariant under the group (3.5). If δ_1 is not properly chosen, (3.4) becomes singular when Λ_0 equals any of the relative extrema of the function $\theta_0=\theta_0(s)$. A proper choice of δ_1 is made if, for example, it is taken as an unknown by imposing an additional condition on g_1. We chose the additional condition

$$g_1(0)=0 \tag{3.10}$$

which is invariant under the group (3.5).

When using the variables

$$\omega_1 = -(j+1)xg_1', \qquad \theta_1 = g_1, \tag{3.11}$$

which are invariant under (3.5), the problem posed by (3.4) and (3.10) is written as

$$\frac{d\omega_1}{ds} = (1-j^2)\frac{\omega_1}{\omega_0} + (1+j)^2\frac{\theta_0\theta_1}{\omega_0} + 2\omega_0, \qquad \frac{d\theta_1}{ds} = -\frac{\omega_1}{\omega_0},$$

$$\lim \frac{\omega_1}{4(j+1)s^2} = -\lim \frac{\theta_1}{s^2} = \frac{1}{3+j} \quad \text{as } s \to 0^+,$$

$$\omega_1 = -(j+1)g_1'(1), \quad \theta_1 = g_1(1) \quad \text{at } s = g_0(0). \tag{3.12}$$

For $s \to \infty$, the following asymptotic behavior is found:

$$j=0: \quad \frac{\omega_1}{(s^2 \ln s)} \to 1, \qquad \frac{\theta_1}{(s^2 \ln s)} \to -1,$$

$$j=1: \quad \frac{\omega_1}{s} \to 16, \qquad \frac{\theta_1}{s^2} \to -1,$$

$$j=2: \quad \omega_1 \to 0, \qquad \theta_1 \to -4.$$

Now, from (2.4), (3.1), (3.2), (3.9) and (3.12), the following parametric representation of the response curve is readily obtained:

$$\phi^2 = (\gamma\beta)^{-1}\theta_0(\bar{s})\{1 + (\gamma\beta)^{-1}[2\beta - a + \beta\theta_1(\bar{s})] + \cdots\}, \tag{3.13}$$

$$\psi = (\gamma\beta)^{-1}\omega_0(\bar{s}) + (\gamma\beta)^{-2}[(2\beta - a)\omega_0(\bar{s}) + \beta\omega_1(\bar{s})] + \cdots \tag{3.14}$$

where $\bar{s} = g_0(0)$. The upper multiplicity bound, or ignition limit, ϕ_E is the value of ϕ which is obtained for $\bar{s} = \bar{s}_I$, where $\bar{s}_I$ is the value of $\bar{s}$ at the first maximum of the function $\theta_0 = \theta_0(\bar{s})$ ($s_I = 1.187$, 1.386 and 1.608 for $j = 0$, 1 and 2):

$$j=0: \quad \phi_I^2 = 0.879(\gamma\beta)^{-1}[1 + (\gamma\beta)^{-1}(2\beta - a - 0.952\beta) + \cdots], \tag{3.15}$$

$$j=1: \quad \phi_I^2 = 2.000(\gamma\beta)^{-1}[1 + (\gamma\beta)^{-1}(2\beta - a - 0.910\beta) + \cdots],$$

$$j=2: \quad \phi_I^2 = 3.322(\gamma\beta)^{-1}[1 + (\gamma\beta)^{-1}(2\beta - a - 0.869\beta) + \cdots]. \tag{3.16}$$

The concentration profile for a point of the response curve, i.e. for a value of $\bar{s}$ in (3.13)–(3.14), may be also found from (3.2), (3.6), (3.9), (3.11) and (3.12). It is given parametrically by

$$y = 1 - (\gamma\beta)^{-1}(\bar{s} - s) - (\gamma\beta)^{-2}[(2\beta - a)(\bar{s} - s) + \beta(\bar{s} - s)^2] + \cdots,$$

$$x = \left[\frac{\theta_0(s)}{\theta_0(\bar{s})}\right]^{1/2} \exp\left[\frac{(\bar{s} - s)}{2}\right] \quad \text{for } s \in [0, \bar{s}].$$

The asymptotics (3.13)–(3.14) break down as $\bar{s} \to \infty$, which occurs, in Fig. 1, as one ascends the segment IA for $j = 0$, 1, and as one approaches the point A for $j = 2$. Since this breaking down occurs, for $j = 2$, at a position which approaches A as $\gamma\beta \to \infty$, the maximum number of solutions of (2.7)–(2.8), i.e. the number of turns of the response curve around A, is expected to increase for increasing values of $\gamma\beta$.

4. The extinction regime. The solution in this regime provides the part PC of the response curve in Fig. 1. The asymptotic analysis to be used here is of a type which is well known in the combustion literature (large activation energy asymptotics,

see Clarke [14]), and quite similar to that presented in [6], [7] and [8] for Arrhenius kinetics. For the sake of brevity only the results will be given.

A typical concentration profile consists of three separate parts: a reaction region, for $|x-x_r| \sim (\gamma\beta)^{-1}$, where $y \sim (\gamma\beta)^{-1}$, an internal equilibrium region, for $0 \leqq x < x_r$, where $\gamma\beta y$ vanishes to the leading order in $(\gamma\beta)^{-1}$, and an external frozen region, for $x_r < x \leqq 1$, where $y \sim 1$ and the reaction term vanishes to all algebraic orders in $(\gamma\beta)^{-1}$. Matching between the reaction and frozen regions yields

$$\phi^2 = \lambda^{-2}\Delta_0[1+(\gamma\beta)^{-1}\delta_1+\cdots], \tag{4.1}$$

$$\psi = \frac{1}{1-x_r} \quad \text{if } j=0, \qquad \psi = \frac{-2}{\ln x_r} \quad \text{if } j=1, \qquad \psi = \frac{3x_r}{1-x_r} \quad \text{if } j=2, \tag{4.2}$$

where

$$\Delta_0 = \frac{\psi^2 x_r^{-2j}}{2(j+1)^2 A_{np}}, \tag{4.3}$$

$$\delta_1 = \frac{2j(1+\beta)^2 B_{np}}{x_r\sqrt{2\Delta_0 A_{np}}} + \frac{\beta(1+\beta)A_{n+2,p}+p\gamma_a\beta A_{n+2,p+1}}{A_{np}},$$

$$\lambda^2 = (k+1)^p\left(\frac{(1+\beta)^2}{\gamma\beta}\right)^{n+1-p}\cdot\exp\left(\frac{(\gamma+p\gamma_a)\beta}{1+\beta}\right), \tag{4.4}$$

$$\mu = \frac{k\gamma\beta}{(1+\beta)^2}\exp\left(\frac{\gamma_a\beta}{1+\beta}\right),$$

$$A_{np} = f_{np}(\mu,\infty), \qquad f_{np}(\mu,z) = \int_0^z \frac{u^n\exp(-u)}{(\mu+u)^p}\,du, \tag{4.5}$$

$$B_{np} = \int_0^\infty \left(\sqrt{\frac{f_{np}(\mu,z)}{A_{np}}}-1\right)dz.$$

(4.1) and (4.2) give ϕ^2 and ψ in terms of the reaction region location x_r and can be seen as a parametric representation of the response curve $\psi-\phi$. (4.1) shows that, for $j=1$ and 2 there is a minimum value of ϕ, corresponding to $x_r = e^{-1}$ and $x_r = \frac{1}{2}$ respectively, and given by

(4.6)

$$j=1: \quad \phi_E^2 = \frac{(e/\lambda)^2}{2A_{np}}\left(1+\frac{1}{\gamma\beta}\left(2(1+\beta)^2B_{np}+\frac{\beta(1+\beta)A_{n+2,p}+p\gamma_a\beta A_{n+2,p+1}}{A_{np}}\right)+\cdots\right),$$

$$j=2: \quad \phi_E^2 = \frac{8\lambda^{-2}}{A_{np}}\left(1+\frac{1}{\gamma\beta}\left(2(1+\beta)^2B_{np}+\frac{\beta(1+\beta)A_{n+2,p}+p\gamma_a\beta A_{n+2,p+1}}{A_{np}}\right)+\cdots\right).$$

For $j=0$, ϕ depends monotonously on x_r and its minimum is reached at $x_r=0$ (negative values of x_r have no meaning). However, (4.1) has been obtained with matching conditions at the left of the reaction region which are valid only if $x_r \gg (\gamma\beta)^{-1}$. Therefore, the precise determination of the lower multiplicity bound, or extinction limit, ϕ_E, requires us to analyze the problem more carefully if $j=0$, as will be done in § 5.

For $j=1$ and 2, the asymptotics (4.1) break down as $x_r \to 0$, which occurs in Fig. 1 as one descends the segment EC and comes into the middle regimes, which will be analyzed for cylinders in § 6. The description of the spiral part AC of the response curve for spheres, which is similar to that of the case $p=0$ (see [8]), will be omitted

for the sake of brevity. For $j=0$, 1 and 2, the analysis above remains valid when x_r approaches 1, as may be easily seen; therefore, (4.1)–(4.2) give the upper branch of the response curve in Fig. 1 also for $\phi^2 \to \infty$.

The concentration at the center, $y(0)$, is determined below from a more detailed analysis of the equilibrium region. For matching purposes we need the asymptotic behavior of the solution at the left of the reaction region, which is given by

$$n=1: \quad z=\exp\left(\sqrt{\frac{\Delta_0}{\mu^p}}\left(\xi-\frac{a_p+b_p}{\sqrt{2\Delta_0}}\right)+o(1)\right)+O(\gamma\beta)^{-1} \quad \text{as } \xi\to-\infty, \tag{4.7}$$

$$n>1: \quad z=\left(\frac{1-n}{2}\sqrt{\frac{2\Delta_0}{(n+1)\mu^p}}\,\xi+o(\xi)\right)^{2/(1-n)}+O(\gamma\beta)^{-1} \quad \text{as } \xi\to-\infty \tag{4.8}$$

where

$$a_p=\int_0^1\left(\frac{\sqrt{2\mu^p}}{z}-\frac{1}{\sqrt{f_{1p}(\mu,z)}}\right)dz,$$
$$b_p=\int_1^\infty\left(\frac{1}{\sqrt{A_{1p}}}-\frac{1}{\sqrt{f_{1p}(\mu,z)}}\right)dz+\frac{1}{\sqrt{A_{1p}}}. \tag{4.9}$$

The inner variables in the reaction region, z and ξ, are

$$z=\frac{\gamma\beta}{(1+\beta)^2}y, \qquad \xi=\frac{\gamma\beta}{(1+\beta)^2}(x-x_r). \tag{4.10}$$

4.1. Concentration at the center of the particle. For simplicity in the presentation we consider only the spherical geometry, $j=2$. It is necessary to distinguish two cases: $n=1$ and $n>1$.

If $n=1$, the concentration is exponentially small in the equilibrium region. (2.7) and the boundary condition at $x=0$ may be written in this region as

$$\frac{d^2z}{d\zeta^2}+\frac{2}{\zeta}\frac{dz}{d\zeta}=z+O(z^2), \qquad \frac{dz}{d\zeta}=0 \quad \text{at } \zeta=0, \tag{4.11}$$

where z is given by (4.10) and

$$\zeta=\frac{\gamma\beta}{(1+\beta)^2}\sqrt{\frac{\Delta_0}{\mu^p}}\left(1+(\gamma\beta)^{-1}\frac{\delta_1}{2}+\cdots\right)x.$$

Since z vanishes to any algebraic order in $(\gamma\beta)^{-1}$ in this region—see (4.13) below—$O(z^2)$ can be ignored in (4.11), whose solution is then

$$z=z(0)\zeta^{-1}Sh\zeta. \tag{4.12}$$

Matching of (4.7) and (4.12) yields

$$y(0)=2\sqrt{\frac{\Delta_0}{\mu^p}}x_r\exp\left(-\sqrt{\frac{\Delta_0}{\mu^p}}\left(\frac{\gamma\beta}{(1+\beta)^2}x_r+\frac{1}{2}\frac{\delta_1 x_r}{(1+\beta)^2}+\frac{a_p+b_p}{\sqrt{2\Delta_0}}\right)+O(\gamma\beta)^{-1}\right) \tag{4.13}$$

where the definition (4.10) of z has been taken into account. Δ_0, δ_1, a_p and b_p are given by (4.3) and (4.9). (4.13) shows that, if $\mu\to 0$,

$$y(0)\sim\exp\left(-\frac{\gamma\beta/(1+\beta)^2}{(1-x_r)\sqrt{2\mu^p A_{1p}}}\right).$$

Since $\mu^p A_{1p} \to 0$, the concentration at the center takes extremely small values if μ is small (i.e. K_a is large). This fact explains the numerical difficulties encountered by Pereira and Varma [5] in this regime.

If $n > 1$, (2.7) and the boundary condition at $x = 0$ may be written, in the equilibrium region, as

$$\frac{d^2 v_0}{d\eta^2} + \frac{2}{\eta}\frac{dv_0}{d\eta} = v_0^n, \qquad v_0(0) = 1, \quad v_0'(0) = 0 \tag{4.14}$$

where

$$v_0 = \frac{y}{y(0)} + O(\alpha), \quad \eta = x\left(\frac{\gamma\beta}{(1+\beta)^2}\right)^{(n+1)/2} \sqrt{\frac{\Delta_0}{\mu^p}}\,(y(0))^{(n-1)/2}(1+O(\alpha)) \tag{4.15}$$

and $\alpha = (\gamma\beta)^{-1}$, $(\gamma\beta)^{-1}\ln(\gamma\beta)$ or $(\gamma\beta)^{2/(1-n)}$ depending on whether $1 < n < 3$, $n = 3$ or $n > 3$, as obtained by higher order matching considerations.

The solution of the initial value problem (4.14) becomes unbounded as η approaches a certain value $\eta_r = \eta_r(n)$. The asymptotic behavior of v_0, for $\eta \to \eta_r^-$, is found to be

$$v_0 = \left(\frac{2(n+1)}{(n-1)^2}(\eta_r - \eta)^{-2}\right)^{1/(n-1)} (1 + O(\eta_r - \eta)). \tag{4.16}$$

Matching of (4.8) and (4.16), via the definitions (4.10) and (4.15), yields

$$y(0) = \left(\frac{(1+\beta)^2}{\gamma\beta}\right)^{(n+1)/(n-1)} \left(\frac{\mu^p \eta_r^2}{\Delta_0 x_r^2}\right)^{1/(n-1)} (1 + O(\alpha)).$$

5. Extinction for slabs. The part BD of the response curve in Fig. 1 will be described now. The concentration profiles are to be as those encountered in § 4. The equilibrium and reaction regions will be coupled and a detailed analysis of the former will be necessary to calculate the response curve, which will be described in terms of the concentration at the center of the particle. We shall distinguish two cases, $n = 1$ and $n > 1$.

5.1. The case $n = 1$. The response curve will be described in terms of the parameter

$$t = \frac{(\gamma\beta)^{3/2}}{(1+\beta)^2}\frac{y(0)}{\mu}.$$

Then ψ, ϕ^2 and the location of the reaction region x_r are considered as unknowns. We shall seek the expansions

$$\psi = \left(\frac{dy}{dx}\right)_{x=1} = 1 + \psi_1 \frac{\ln(\gamma\beta)}{\gamma\beta} + \frac{\psi_2}{\gamma\beta} + \cdots, \tag{5.1}$$

$$\phi^2 = \lambda^{-2}\Delta_0\left(1 + \delta_1 \frac{\ln\gamma\beta}{\gamma\beta} + \frac{\delta_2}{\gamma\beta} + \cdots\right), \tag{5.2}$$

$$x_r = \sqrt{\frac{\mu^p}{\Delta_0}}\frac{(1+\beta)^2}{\gamma\beta}\left(\frac{1}{2}\ln\gamma\beta + \Omega_1 + \frac{\Omega_2}{\sqrt{\gamma\beta}} + \cdots\right) \tag{5.3}$$

where λ^2 is given by (4.4). A part of the matching conditions among the three regions is anticipated in the form of the expansions (5.1)–(5.3).

Equilibrium region. When using the variables

$$w = \frac{(\gamma\beta)^{3/2}}{(1+\beta)^2}\frac{y}{\mu}, \qquad \zeta = \frac{\gamma\beta}{(1+\beta)^2}x$$

(2.7) and its boundary conditions at $x = 0$ can be written as

$$\frac{d^2w}{d\zeta^2} = \frac{\Delta_0}{\mu^p}w\left(1-(\mu+p)\frac{w}{\sqrt{\gamma\beta}}+\delta_1\frac{\ln(\gamma\beta)}{\gamma\beta}+\frac{2\delta_2+(p^2+\mu^2+2p\mu+p)w^2}{2\gamma\beta}+\cdots\right),$$

$$w(0) = t, \qquad w'(0) = 0.$$

This initial value problem has a closed-form solution. Its asymptotic behavior for large ζ, i.e. for large w, is found to be

$$\zeta = \sqrt{\frac{\mu^p}{\Delta_0}}\left(\ln\frac{2w}{t}-\frac{t^2}{4w^2}+\cdots+\frac{1}{\sqrt{\gamma\beta}}\frac{\mu+p}{3}\left(wt+\frac{t}{2}+\cdots\right)\right.$$

(5.4)

$$\left.-\frac{\ln(\gamma\beta)}{\gamma\beta}\frac{\delta_1}{2}\left(\ln\frac{2w}{t}+\cdots\right)+\frac{1}{\gamma\beta}\left(\frac{(\mu+p)^2}{6}w^2+\cdots\right)+\cdots\right).$$

Reaction region. Equation (2.7) can be written as

$$\frac{d^2z}{d\xi^2} = \Delta_0\frac{z\,e^{-z}}{(\mu+p)^2}\left(1+\delta_1\frac{\ln(\gamma\beta)}{\gamma\beta}+\frac{1}{\gamma\beta}\left(\delta_2-\beta(1+\beta)z^2-p\gamma_a\beta\frac{z^2}{\mu+z}\right)+\cdots\right)$$

in terms of the variables z and ξ, given by (4.10). This equation can be solved by quadratures. After introducing the appropriate constants of integration for the matching with the equilibrium region to be possible, the following asymptotic behaviors are found:

$$\xi = \sqrt{\frac{\mu^p}{\Delta_0}}\ln z+\alpha_0+\frac{a_p}{\sqrt{2\Delta_0}}+\cdots+\frac{\alpha_1}{\sqrt{\gamma\beta}}+\alpha_2\frac{\ln^2(\gamma\beta)}{\gamma\beta}$$

(5.5)

$$-\frac{\ln(\gamma\beta)}{\gamma\beta}\left(\frac{\delta_1}{2}\sqrt{\frac{\mu^p}{\Delta_0}}\ln z+\cdots\right)+\frac{1}{\gamma\beta}\left(\frac{\alpha_3}{2}\left(\frac{\mu^p}{\Delta_0}\right)^{3/2}z^{-2}+\cdots\right)+\cdots$$

as $z \to 0$,

$$\xi = \frac{z}{\sqrt{2\Delta_0 A_{1p}}}+\alpha_0-\frac{b_p}{\sqrt{2\Delta_0}}+\cdots+\frac{\alpha_1}{\sqrt{\gamma\beta}}+\alpha_2\frac{\ln^2(\gamma\beta)}{\gamma\beta}$$

(5.6)

$$-\frac{\ln(\gamma\beta)}{\gamma\beta}\left(\frac{\delta_1}{2}\frac{z}{\sqrt{2\Delta_0 A_{1p}}}+\cdots\right)$$

$$+\frac{1}{\gamma\beta}\left(\frac{\beta(1+\beta)\Delta_0 A_{3p}+p\gamma_a\beta\Delta_0 A_{3,p+1}-\delta_2\Delta_0 A_{1p}-\alpha_3}{(2\Delta_0 A_{1p})^{3/2}}z+\cdots\right)+\cdots$$

as $z \to \infty$

where A_{np}, a_p and b_p are given by (4.5) and (4.9). Matching of (5.4) and (5.5) yields

$$\alpha_0+\frac{a_p}{\sqrt{2\Delta_0}} = -\sqrt{\frac{\mu^p}{\Delta_0}}\left(\Omega_1+\ln\left(\frac{\mu t}{2}\right)\right), \qquad \frac{\alpha_3\mu^p}{2\Delta_0} = -\frac{\mu^2t^2}{4}. \tag{5.7}$$

Two additional relations involving α_1 and α_2 are not written here; they would be necessary only if higher order terms in the expansions (5.1)–(5.3) were considered.

Frozen region. Since the second member of (2.7) vanishes to any algebraic order in $(\gamma\beta)^{-1}$, for $x_r \leqq x \sim 1$, (2.7) and the boundary condition at $x = 1$ are written as

$$\frac{d^2y}{dx^2} = 0, \qquad y(1) = 1. \tag{5.8}$$

Matching between the solution of (5.8):

$$y = x + (x-1)\left(\psi_1 \frac{\ln \gamma\beta}{\gamma\beta} + \frac{\psi_2}{\gamma\beta} + \cdots\right)$$

and (5.6)—via the definitions (4.10) and (5.2)—leads to

$$\sqrt{2\Delta_0 A_{1p}} = 1, \qquad \psi_1 = \frac{\delta_1}{2} = \frac{(1+\beta)^2}{2}\sqrt{\frac{\mu^p}{\Delta_0}}, \tag{5.9}$$

$$\begin{aligned}\psi_2 &= \frac{\delta_2}{2} + \alpha_3 - \beta(1+\beta)\frac{A_{3p}}{2A_{1p}} - p\gamma_a\beta\frac{A_{3,p+1}}{2A_{1p}} \\ &= (1+\beta)^2\left(\sqrt{\frac{\mu^p}{\Delta_0}}\,\Omega_1 + \alpha_0 - \frac{b_p}{\sqrt{2\Delta_0}}\right).\end{aligned} \tag{5.10}$$

From (5.7), (5.9) and (5.10) we get

$$\Delta_0 = (2A_{1p})^{-1}, \qquad \delta_1 = 2\psi_1 = (1+\beta)^2\sqrt{2\mu^p A_{1p}},$$

$$\delta_2 = 2\psi_2 + \frac{\mu^2 t^2}{2\mu^p A_{1p}} + \beta(1+\beta)\frac{A_{3p}}{A_{1p}} + p\gamma_a\beta\frac{A_{3,p+1}}{A_{1p}},$$

$$\psi_2 = -(1+\beta)^2\sqrt{A_{1p}}\left(a_p + b_p + \sqrt{2\mu^p}\ln\frac{\mu t}{2}\right).$$

A further substitution into (5.1) and (5.2) gives a parametric representation of the response curve, which is as the branch *BD* in Fig. 1. The minimum of δ_2, corresponding to $t_E = (2A_{1p})^{3/4}(1+\beta)\cdot\mu^{(3p-4)/4}$, gives the extinction limit

$$\begin{aligned}\phi_E^2 = \frac{\lambda^{-2}}{2A_{1p}}\Bigg(&1 + (1+\beta)^2\sqrt{2\mu^p A_{1p}}\,\frac{\ln(\gamma\beta)}{\gamma\beta} \\ &+ \frac{1}{\gamma\beta}\left(\beta(1+\beta)\frac{A_{3p}}{A_{1p}} + p\gamma_a\beta\frac{A_{3,p+1}}{A_{1p}} + \frac{\mu^2 t_E^2}{2\mu^p A_{1p}}\right. \\ &\left. - 2(1+\beta)^2\sqrt{A_{1p}}\left(a_p + b_p + \sqrt{2\mu^p}\ln\frac{\mu t_E}{2}\right)\right) + \cdots\Bigg).\end{aligned} \tag{5.11}$$

5.2. The case $n > 1$. The analysis is similar to that of the case $n = 1$. The response curve is described in terms of the parameter

$$t = y(0)\varepsilon^{-3/2};$$

ψ, ϕ^2 and x_r are expanded as

$$\psi = \psi_0 + \varepsilon\psi_1 + \cdots, \quad \phi^2 = \lambda^{-2}\Delta_0(1 + \varepsilon\delta_1 + \cdots), \quad x_r = \varepsilon(\zeta_r + \cdots) \tag{5.12}$$

where λ is given by (4.4), and

$$\varepsilon = \left(\frac{(1+\beta)^2}{\gamma\beta}\right)^{2(n+1)/(3n+1)}$$

In the *equilibrium region*, (2.7) and the boundary conditions at $x = 0$ are

$$\frac{d^2w}{d\zeta^2} = \frac{\Delta_0 w^n}{\mu^p}(1+\cdots), \quad w = t, \quad \frac{dw}{d\zeta} = 0 \quad \text{at } \zeta = 0, \tag{5.13}$$

where

$$w = \varepsilon^{-3/2} y, \qquad \zeta = \varepsilon^{-1} x.$$

The asymptotic behavior, as $w \to \infty$, of the solution of (5.13) is

$$\zeta = \sqrt{\frac{(n+1)\mu^p}{2\Delta_0}}\left(c_n t^{(1-n)/2} - \frac{2w^{(1-n)/2}}{n-1} - \frac{t^{n+1} w^{-(3n+1)/2}}{3n+1} + \cdots\right) \tag{5.14}$$

where

$$c_n = \int_1^\infty (w^{n+1} - 1)^{-1/2}\, dw.$$

In the *reaction region*, (2.7) can be written as

$$\frac{d^2z}{d\xi^2} = \frac{\Delta_0 z^n e^{-z}}{(\mu+z)^p}(1+\varepsilon\delta_1+\cdots) \tag{5.15}$$

in terms of the variables z and ξ, given by (4.10). The asymptotic behavior, as $z \to 0$, of the solution of (5.15) is

$$\begin{aligned}\xi = &-\frac{2}{n-1}\sqrt{\frac{(n+1)\mu^p}{2\Delta_0}}\, z^{(1-n)/2} + \cdots \\ &+\varepsilon\left(\frac{2\alpha_1}{3n+1}\left(\frac{(n+1)\mu^p}{2\Delta_0}\right)^{3/2} z^{-(3n+1)/2} + \cdots\right) + \cdots .\end{aligned} \tag{5.16}$$

Matching with (5.14) yields

$$\zeta_r = \sqrt{\frac{(n+1)\mu^p}{2\Delta_0}}\, c_n t^{(1-n)/2}, \qquad \alpha_1 = -\frac{\Delta_0}{(n+1)\mu^p}\, t^{n+1}. \tag{5.17}$$

The asymptotic behavior, as $z \to \infty$, of the solution of (5.15) is

$$\xi = \frac{z}{\sqrt{2\Delta_0 A_{np}}} + \cdots - \varepsilon\left(\frac{\alpha_1 + \delta_1 \Delta_0 A_{np}}{(2\Delta_0 A_{np})^{3/2}}\zeta + \cdots\right) + \cdots .$$

In the *frozen region*, (2.7) and the boundary condition at $x = 1$ are again (5.8), which has a solution

$$y = x + \varepsilon\psi_1(x-1) + \cdots .$$

Matching with (5.16) yields

$$\sqrt{2\Delta_0 A_{np}} = 1, \qquad \psi_1 = \zeta_r = \alpha_1 + \frac{\delta_1}{2}; \tag{5.18}$$

(5.17) and (5.18) give ψ_1, Δ_0 and δ_1 in terms of t. A further substitution into (5.12) leads to the representation of the response curve:

$$\psi = 1 + \varepsilon\sqrt{\frac{(n+1)\mu^p}{2\Delta_0}}\, c_n t^{(1-n)/2} + \cdots ,$$

$$\phi^2 = \frac{\lambda^{-2}}{2A_{np}}\left(1 + \varepsilon\left(2\sqrt{(n+1)\mu^p A_{np}}\, c_n t^{(1-n)/2} + \frac{t^{n+1}}{(n+1)\mu^p A_{np}}\right) + \cdots\right).$$

The minimum of ϕ^2, corresponding to

$$t_E = ((n+1)(n-1)^2 \mu^{3p} A_{np}^3 c_n^2)^{1/(3n+1)} + \cdots,$$

gives the extinction limit ϕ_E.

6. The intermediate regimes for cylinders. The concentration at the center of the particle, $y(0)$, was close to 1 in the ignition regime, and it was small compared with $(\gamma\beta)^{-1}$ in the extinction regime. Intermediate values of $y(0)$ will be considered now. The distinguished limits $y(0) \sim 1$ and $y(0) \sim (\gamma\beta)^{-1}$ will be treated separately. If $\mu \sim \gamma\beta$ the response curve differs only quantitatively from that of the Arrhenius kinetics case, and the solution is unique in those regimes (see [7]). We shall consider smaller values of μ, i.e., $\mu = o(\gamma\beta)$. It will be assumed that $\beta = o(1)$ to simplify the presentation of the analysis.

6.1. Lower intermediate regime. In this regime, the concentration at the center is

$$y(0) = y_0 \gg (\gamma\beta)^{-1}$$

and ϕ is such that the parameter

$$\bar{\alpha}^2 = \frac{y_0^{p-n}}{\phi^2 (k+1)^p} \frac{(1+\beta(1-y_0))^2}{\gamma\beta} \exp\left(-\frac{(\gamma + p\gamma_a)\beta(1-y_0)}{1+\beta(1-y_0)}\right) \tag{6.1}$$

vanishes to any algebraic order in $(\gamma\beta)^{-1}$.

The concentration profiles consist of two regions. In an *inner core*, the inner variables

$$\zeta = \frac{x}{\bar{\alpha}}, \qquad z = \frac{\gamma\beta(y-y_0)}{(1+\beta(1-y_0))^2}$$

are used to write (2.7) and the boundary conditions at $x = 0$ as

$$\frac{d^2 z}{d\zeta^2} + \frac{1}{\zeta}\frac{dz}{d\zeta} = e^{-z}\left(1 + \frac{(n-p)z - p\mu}{\gamma\beta y_0} + \cdots\right), \qquad z = \frac{dz}{d\zeta} = 0 \quad \text{at } \zeta = 0. \tag{6.2}$$

(6.2) can be solved by quadratures. Its asymptotic behavior, as $\zeta \to \infty$, is found to be

$$z = 4\ln\zeta - 2\ln 8 + \cdots + (\gamma\beta)^{-1}\left(4\frac{n-p}{y_0}\ln\zeta + \cdots\right) + \cdots. \tag{6.3}$$

In an outer *frozen region*, $y \sim x \sim 1$, the second member of (2.7) is exponentially small. When taking into account the boundary condition $y(1) = 1$, the solution in this region is found to be

$$y = 1 + \psi\frac{\ln x}{2} + \cdots. \tag{6.4}$$

Matching with (6.3) yields

$$\psi = 8\frac{(1+\beta(1-y_0))^2}{\gamma\beta}\left(1 + \frac{n-p}{\gamma\beta y_0} + \cdots\right), \tag{6.5}$$

$$\bar{\alpha}^2 = \frac{1}{8}\exp\left(-\frac{(\gamma\beta y_0 + p - n)(1-y_0)}{2(1+\beta(1-y_0))^2 y_0}\right)(1 + \cdots). \tag{6.6}$$

Substitution of (6.6) into (6.1) leads to

$$\phi^2 = \frac{8y_0^{n-p}}{\gamma\beta} \exp\left(\frac{(\gamma\beta y_0 + p - n)(1-y_0)}{2(1+\beta(1-y_0))^2 y_0} - \frac{\gamma\beta(1-y_0)}{1+\beta(1-y_0)}\right)(1+\cdots). \tag{6.7}$$

(6.5) and (6.7) describe parametrically, through y_0, the branch AB in Fig. 1b, and show that the response curve is monotonous—and therefore the solution is unique—in this regime if $n > p$; if $n < p$, there is a minimum value of ϕ, i.e., a lower multiplicity bound ϕ_m, which corresponds to $y_{0m} = \sqrt{(p-n)/\gamma\beta} + \cdots$.

6.2 Upper intermediate regime. The response curve will be described in terms of the parameter

$$\tau = \frac{(1+\beta)^2}{\gamma\beta} y(0),$$

and ϕ^2 will be such that

$$\bar{\alpha}^2 = \phi^{-2}(k+1)^{-p}\left(\frac{(1+\beta)^2}{\gamma\beta}\right)^{p+1-n} \exp\left(-\frac{(\gamma + p\gamma_a)\beta}{1+\beta}\right) \tag{6.8}$$

vanishes to any algebraic order in $(\gamma\beta)^{-1}$. As in § 6.1, the concentration profiles consist of two regions. In an *inner core*, (2.7) and the boundary conditions at $x = 0$ are written as

$$\frac{d^2z}{d\zeta^2} + \frac{1}{\zeta}\frac{dz}{d\zeta} = \frac{z^n e^{-z}}{(\mu+z)^p}(1+O(\gamma^{-1})), \qquad z = \tau, \quad \frac{dz}{d\zeta} = 0 \quad \text{at } \zeta = 0 \tag{6.9}$$

in terms of the variables $\zeta = x/\bar{\alpha}$ and $z = \gamma\beta y/(1+\beta)^2$.

The asymptotic behavior of the solution of (6.9), as $\zeta \to \infty$, is

$$z = b(\tau)(\ln\zeta - c(\tau)) + o(1). \tag{6.10}$$

In a *frozen region*, $y \sim x \sim 1$, the second member of (2.7) is, as in § 6.1, exponentially small. The solution in this region is given by (6.4) again, and the matching with (6.10) yields

$$\psi = 2\frac{(1+\beta)^2}{\gamma\beta}(b(\tau) + O(\gamma^{-1})),$$

$$\bar{\alpha}^2 = \exp\left(-\frac{\gamma\beta}{(1+\beta)^2}\frac{2}{b(\tau)} - 2c(\tau) + O(\beta)\right). \tag{6.11}$$

Substitution of (6.11) into (6.8) leads to

$$\phi^2 = (\gamma\beta)^{n-p-1} \exp\left(-\frac{\gamma\beta}{1+\beta} + \frac{2\gamma\beta}{(1+\beta)^2 b(\tau)} + 2c(\tau) + O(\beta)\right). \tag{6.12}$$

The analysis of the functions $b = b(\tau)$ and $c = c(\tau)$, in the Appendix, shows that there are multiple solutions in this regime. The response curve is as that in sketch b of Fig. 1. Observe that the number of solutions is arbitrarily large for sufficiently small value of μ and $\phi = \phi_c$, where ϕ_c is posed by (6.12) with $(b, c) = (b_c, c_c)$.

7. The Robin problem. The Robin problem (1.1)–(1.3), under the assumptions (1.4)–(1.5), will be analyzed below. For the sake of brevity, only the spherical geometry ($j = 2$) will be considered. The response curves, which are as those sketched in Fig. 3, are obtained from the results of §§ 3–4, via the transformations defined in § 2.

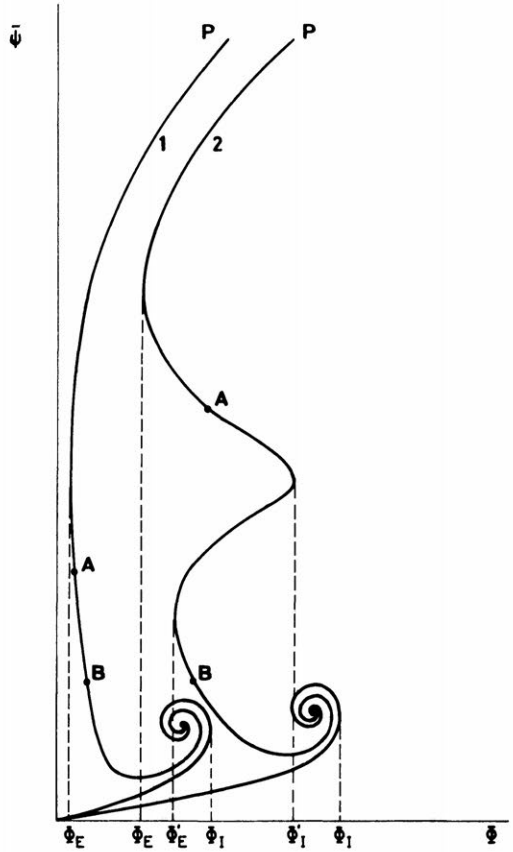

FIG. 3. *Sketch of the response curves for the Robin problem* (1.1)–(1.3) *in spheres and* $d<3$ (*curve* 1) *or* $d>3$ (*curve* 2).

7.1. The ignition regime. This regime appears as $\psi \sim \Phi^2 \sim (\bar{\gamma}\bar{\beta})^{-1}$. A substitution of (2.1), (2.4) and (2.6) into (3.13) and (3.14) yields the following parametric representation of the response curve:

$$\Phi^2 = \frac{(1+K_a)^p}{\bar{\gamma}\bar{\beta}}\,\theta_0(s)\exp\left(-\frac{\omega_0(s)}{3\nu}\right)(1+o(1)), \tag{7.1}$$

$$\bar{\psi} = \frac{\omega_0(s)}{\bar{\gamma}\bar{\beta}}\,(1+o(1)).$$

This representation shows that the response curve in this regime has the same shape as that of the Dirichlet problem. The ignition limit Φ_I is obtained by differentiation of (7.1); it corresponds to $s = s_I + o(1)$, where s_I is the smaller root of the equation

$$\theta_0(s_I) + \frac{\nu-1}{3}\,\omega_0(s_I) = 2\nu. \tag{7.2}$$

A plot of Φ_I vs. ν, as calculated from (7.1) and (7.2), is given in Fig. 4.

7.2. The extinction regimes. There are two distinguished regimes which corresponds to the so-called extinction regime of the Dirichlet problem.

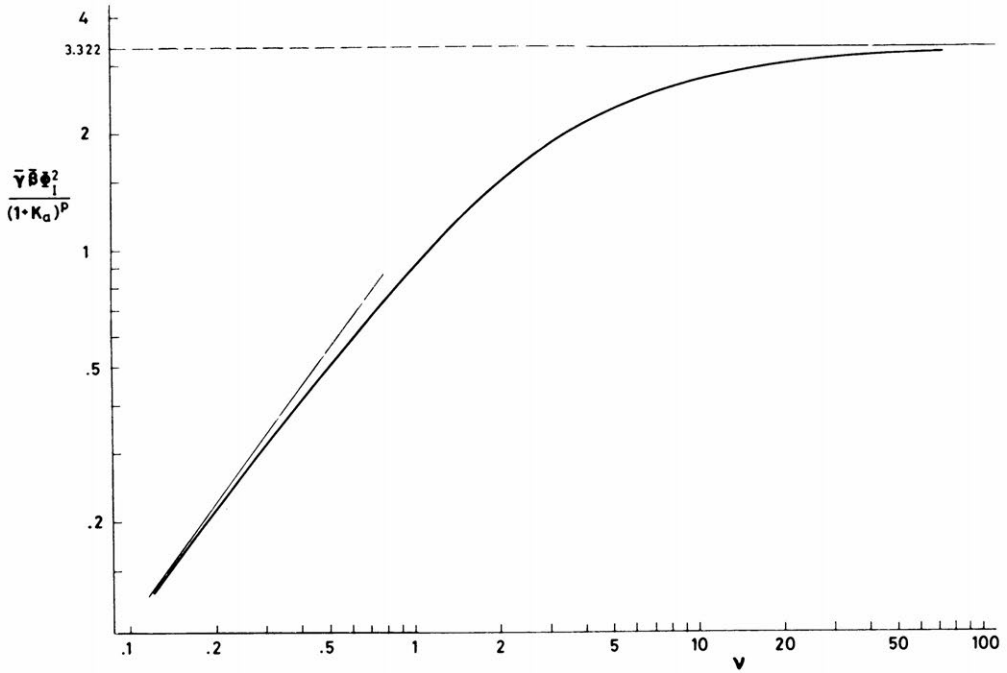

FIG. 4. *Ignition limit for the Robin problem in spheres.*

7.2.1. First extinction regime. The first regime to be considered corresponds to $\psi \ll \sigma$. It gives the part AB of the response curve in Fig. 3. A substitution of (2.1), (2.4) and (2.6) into (4.1) and (4.2), and elimination of the parameter x_r, gives the following representation of the first approximation of the response curve:

$$\Phi^2 = \frac{K_a^p}{6A_{np}(\mu)}\left(\frac{\bar{\gamma}\bar{\beta}}{(1+\bar{\beta})^2}\right)^{n+1-p} \exp\left(-\frac{(\bar{\gamma}+p\bar{\gamma}_a)\bar{\beta}}{1+\bar{\beta}}\right)\frac{(\bar{\psi}+3)^4}{3\bar{\psi}} \exp\left(-\frac{(\bar{\gamma}+p\bar{\gamma}_a)\bar{\beta}}{3(1+\bar{\beta})^2\nu}\bar{\psi}\right)(1+o(1))$$

where

$$\mu = K_a^{-1}\frac{\bar{\gamma}\bar{\beta}}{(1+\bar{\beta})^2}\exp\left(\frac{\bar{\gamma}_a\bar{\beta}}{1+\bar{\beta}}\right).$$

It shows that the solution is unique in this regime if

$$d = \frac{3(1+\bar{\beta})^2\nu}{(\bar{\gamma}+p\bar{\gamma}_a)\bar{\beta}} < 3, \tag{7.3}$$

while there are three solutions of the problem for Φ in a certain interval $]\Phi'_E, \Phi'_I[$ otherwise. The multiplicity bounds Φ'_E and Φ'_I corresponds to $\bar{\psi} = \bar{\psi}_E$ and $\bar{\psi} = \bar{\psi}_I$, where

$$\bar{\psi}_{E,I} = \frac{3(d-1) \pm \sqrt{9d^2-30d+9}}{2}.$$

A plot of the multiplicity bounds vs. d is shown in Fig. 5.

7.2.2. Second extinction regime. The second distinguished regime corresponds to $\psi \sim \sigma \gg 1$. Substitution of (2.1), (2.4) and (2.6) into (2.9) yields, in first approxi-

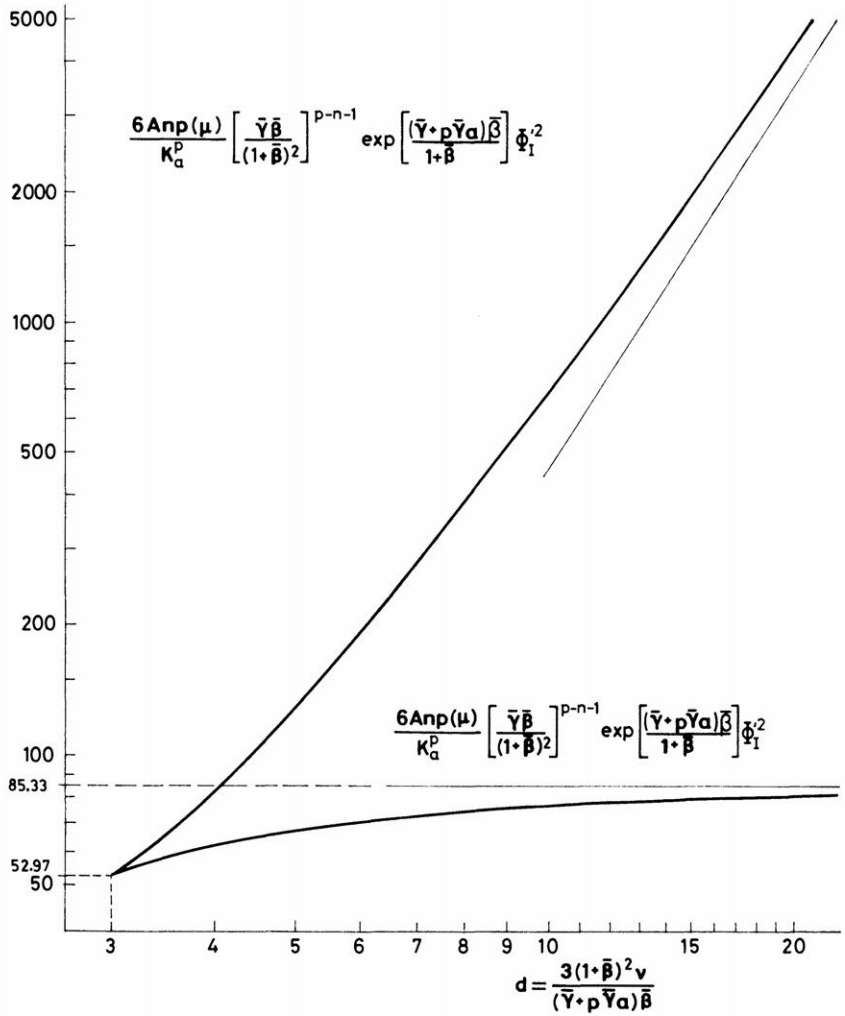

FIG. 5. *Bounds of the multiplicity interval of the first extinction regime for the Robin problem in spheres.*

mation,

$$\Phi^2=\frac{\sigma^2\delta^{n+1}\exp(-\bar\gamma)}{2}\left(\frac{\xi}{1+\xi}\right)^2\frac{\exp(e(1+\xi)/\xi)}{g_{np}(\delta/(1+\xi))}, \tag{7.4}$$

$$\bar\psi=3\sigma\xi \tag{7.5}$$

where

$$\delta=K_a\exp(-\bar\gamma_a),\quad e=\frac{(\bar\gamma+p\bar\gamma_a)\nu}{\bar\beta\sigma},\quad g_{np}(z)=\int_0^z\frac{z^n dz}{(1+z)^p}.$$

(7.4) and (7.5), which give parametrically the part PA of the response curve in Fig. 3, show that there exist no solution if $\Phi<\Phi_E$ and two solutions if $\Phi>\Phi_E$, where Φ_E corresponds to $\xi=\xi_E$, which is given by

$$\frac{2}{\xi_E}-\frac{2}{1+\xi_E}-\frac{e}{\xi_E^2}+\frac{\delta}{(1+\xi_E)^2}\frac{g_{np}'(\delta/(1+\xi_E))}{g_{np}(\delta/(1+\xi_E))}=0.$$

A plot of Φ_E vs. e for representative values of δ, in the case $n = 1$, $p = 2$, is given in Fig. 6.

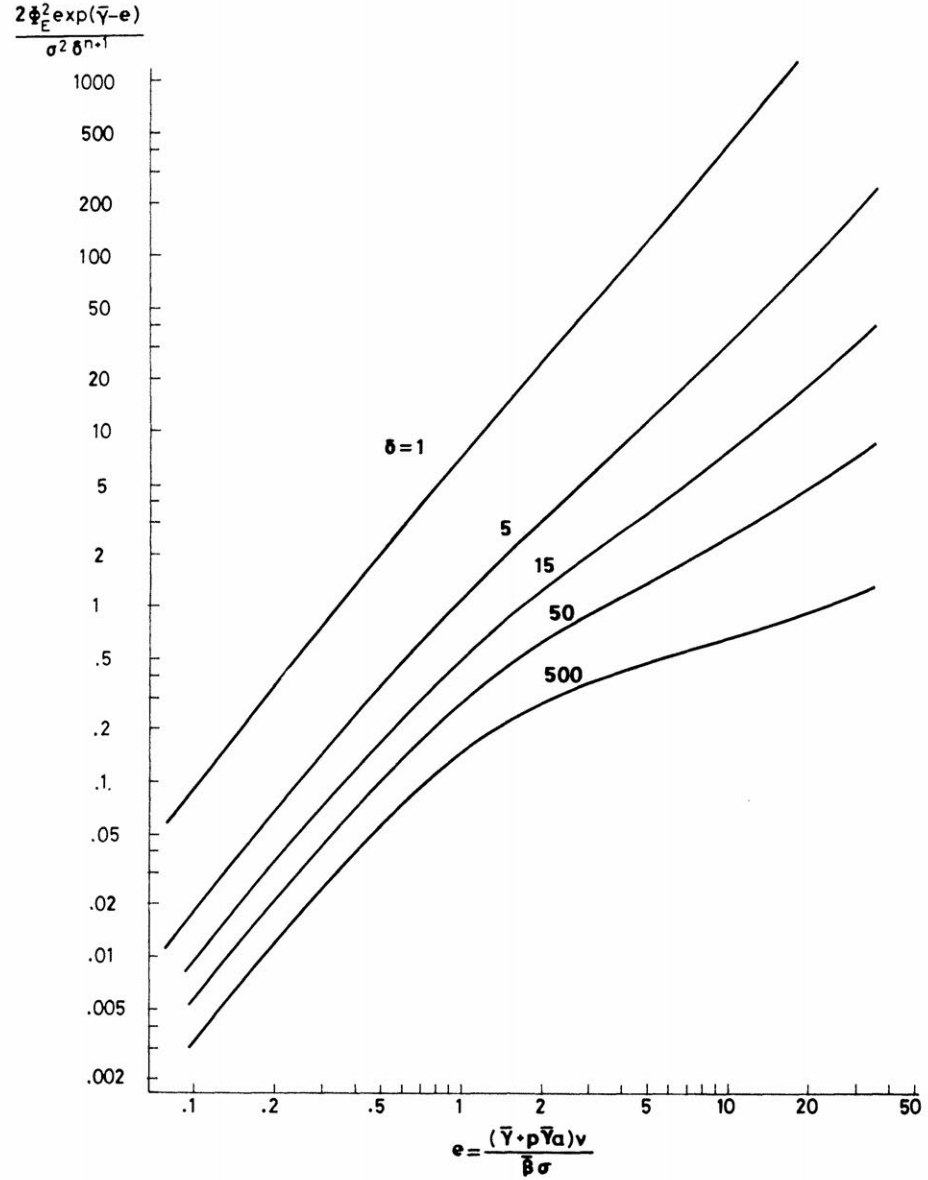

FIG. 6. *Extinction limit for the Robin problem in spheres* ($n = 1$, $p = -2$).

8. Conclusions. An asymptotic analysis of the problem (2.7)–(2.8), for $\gamma\beta \to \infty$, has been carried out in §§ 3–6. It has been shown that the response curve exhibits multiplicity in a certain interval $[\phi_E, \phi_I]$. The response curve is S-shaped for the slab geometry, while for spheres it has a spiral shape, as in the case of Arrhenius kinetics ($p = 0$) and large activation energies. For cylinders, it is S-shaped if $n \geqq p$ or $n < p$ and $k^{-1} = O(1)$; for $n < p$ and $k\gamma\beta = O(1)$ there exists a subinterval of $[\phi_E, \phi_I]$ where the number of solutions is five at least; as $k\gamma\beta \to 0$ the response curve spirals around

a certain point as in the spherical geometry. Observe that this behavior of the response curve matches with the results of [6]–[9].

A comparison between the asymptotic values of the multiplicity bounds ϕ_E and ϕ_I for $j=0$ and 2 (i.e., the two terms expansion posed by (3.15), (3.16), (4.6) and (5.11)) and their numerically computed ones, found in the literature, is plotted in Fig. 7. Observe that the differences are always under 5% in spite of the moderately large value of $\bar{\gamma}\bar{\beta}$.

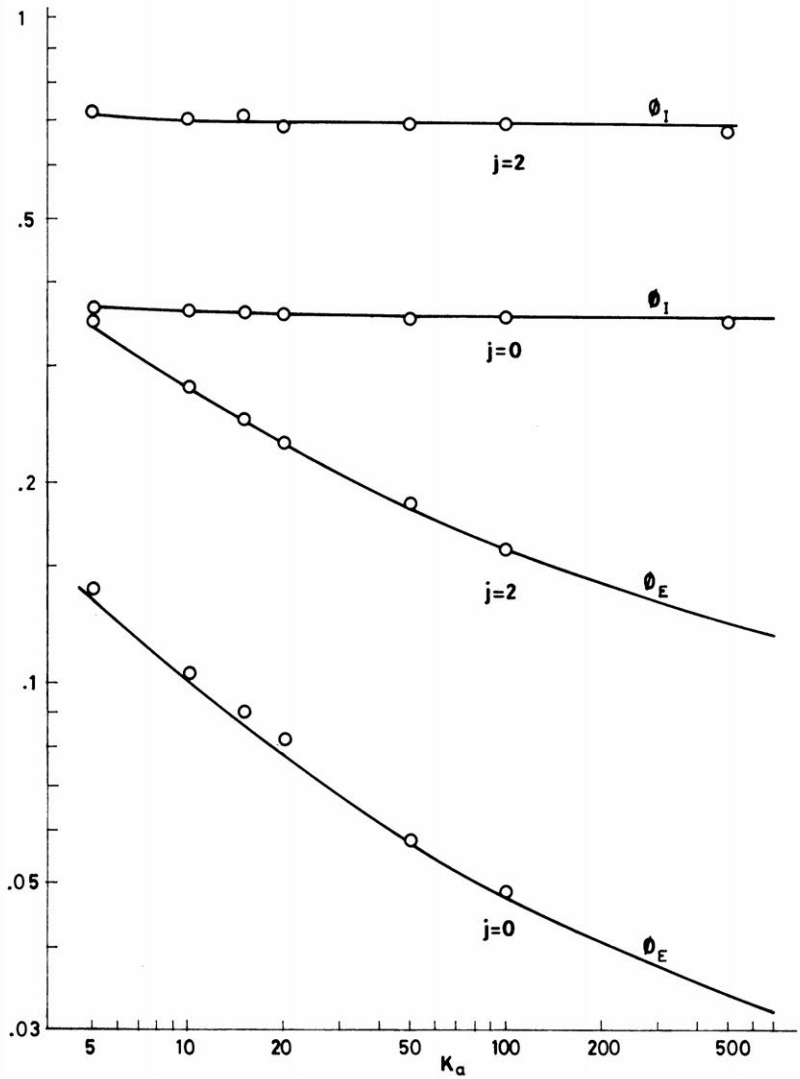

FIG. 7. *Ignition and extinction limits for the Dirichlet problem in the case* $n=1$, $p=2$, $\gamma=30$, $\beta=.2$ *and* $\bar{\gamma}_a=0$ *as calculated in* §§ 3–5 (———) *and as taken from* [5] (○).

For boundary conditions of Robin type, (1.1)–(1.3) have been analyzed in § 7. It has been shown that the upper part of the response curve, which corresponds to the so-called extinction regime, has the same shape as that of the Dirichlet problem or contains an S-shaped part, depending on whether the nondimensional parameter d

(see (7.3)) is smaller or greater than 3. The remaining part of the response curve has the same shape as that of the Dirichlet problem. The bounds of the several multiplicity intervals are plotted in Figs. 4–6.

Appendix. The functions $\tau \to b(\tau)$ and $\tau \to c(\tau)$ are defined as

$$b(\tau) = \lim_{\zeta \to \infty} \frac{z(\zeta)}{\ln \zeta}, \qquad c(\tau) = \lim_{\zeta \to \infty} \left(\ln \zeta - \frac{z(\zeta)}{b(\tau)} \right)$$

where $z = z(\zeta)$ is given by

$$\text{(A.1)} \qquad \frac{d^2 z}{d\zeta^2} + \frac{1}{\zeta} \frac{dz}{d\zeta} = \frac{z^n \exp(-z)}{(\mu + z)^p}; \qquad z = \tau, \quad \frac{dz}{d\zeta} = 0 \quad \text{at } \zeta = 0.$$

A.1. The limit $\mu \to \infty$. As $\mu \to \infty$, it is easily seen that

$$b = 4\left(1 + \mu^{-1}\left(\frac{n}{\tau} - \frac{p}{1+\tau}\right) + \cdots\right),$$

$$c = \frac{\mu\tau}{4} + \frac{p-n}{2} \ln \mu + \frac{\tau}{4}\left(\frac{n}{\tau} - \frac{p}{1+\tau}\right) + \frac{1}{2} \ln \frac{8(1+\tau)^p}{\tau^n} + \cdots.$$

Observe that, for $n < p$, $b = b(\tau)$ has a minimum which is reached at $\tau_m = (\sqrt{p/n} - 1) + \cdots$.

A.2 The limit $\mu \to 0$. The formal limit $\mu \to 0$ leads to the (regular) perturbation scheme

$$\text{(A.2)} \qquad z = z_0 + \mu z_1 + \cdots, \quad b = b_0 + \mu b_1 + \cdots, \quad c = c_0 + \mu c_1 + \cdots$$

where the leading order terms

$$\text{(A.3)} \qquad b_0(\tau) = \lim_{\zeta \to \infty} \frac{z_0(\zeta)}{\ln \zeta}, \qquad c_0(\tau) = \lim_{\zeta \to \infty} \left(\ln \zeta - \frac{z_0(\zeta)}{b_0(\tau)} \right),$$

$$\text{(A.4)} \qquad \frac{d^2 z_0}{d\zeta^2} + \frac{1}{\zeta} \frac{dz_0}{d\zeta} = z_0^{n-p} \exp(-z_0),$$

$$\text{(A.5)} \qquad z_0 = \tau, \quad \frac{dz_0}{d\zeta} = 0 \quad \text{at } \zeta = 0.$$

The curves $b_0 - c_0$ are shown with solid lines in Fig. 8, as obtained from numerical integrations of (A.3)–(A.5), for representative values of $n - p$. If $n - p > 1$, $(b_0, c_0) \to (\infty, \infty)$ as $\tau \to 0$; if $n - p < 1$, $(b_0, c_0) \to (b_{0c}, c_{0c})$, where b_{0c} and c_{0c} corresponds to the solution z_{0c} of (A.4) which satisfies

$$\lim_{\zeta \to 0} (2\zeta/(1 - n - p))^{2/(n-p-1)} z(\zeta) = 1.$$

This critical point of the curve $b_0 - c_0$ is approached with a constant slope if $n - p \geqq 0$; if $n - p < 0$, the curve spirals around the point as $\tau \to 0$.

For $-1 < n - p < 1$, there exists a second type of solutions of (A.1). They consist of three separate regions. In an *internal region*, $\zeta < \zeta_0$, z vanishes to the leading order;

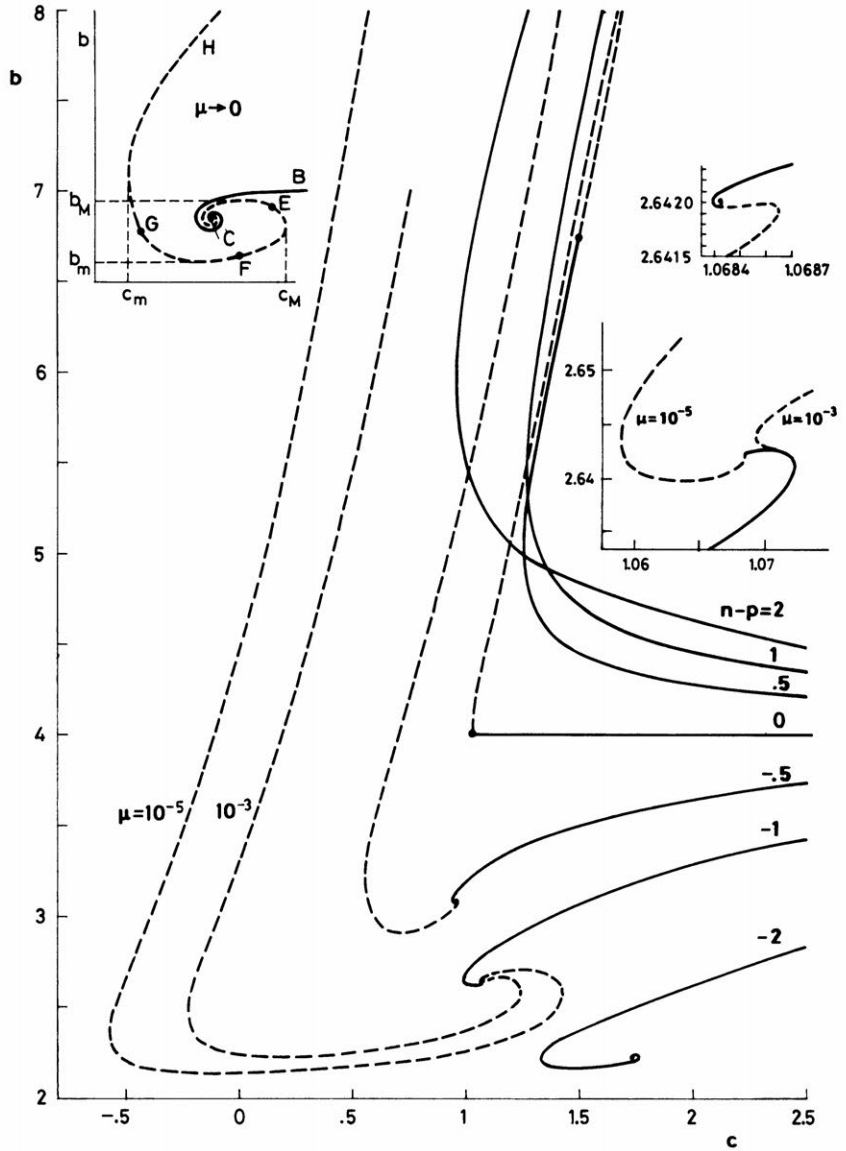

FIG. 8. *The curves* $\tau \to (b(\tau), c(\tau))$ *for* $\mu \to 0$.

in an *external region*, $\zeta > \zeta_0$, and $z = z_0 + o(1)$, where z_0 satisfies (A.4) and

$$z_0 = \frac{dz_0}{d\zeta} = 0 \quad \text{at } \zeta = \zeta_0.$$

These conditions have been obtained from the matching conditions of the two above-mentioned regions with a *thin region* which separates them. The corresponding curves $b_0 - c_0$ are shown with dotted lines in Fig. 8, for representative values of $n - p$. As $\zeta_0 \to 0$, these curves approach the critical point (b_{0c}, c_{0c}), with a constant slope if $n - p \geqq 0$, and with a spiral behavior if $n - p < 0$.

An asymptotic analysis of the case $n-p \leqq -1$ shows that the remaining part of the response curve is as that of the sketch in Fig. 8, consisting of four distinct segments. Observe that the curve $b-c$ has the same shape as that of the case $-1<n-p<0$. The analysis, which is fairly involved, is not presented here for the sake of brevity. Only the results of the limiting case $n-p=-1$ are given:

Segment CE.

$$b=\begin{cases} b_0+O(\ln \varepsilon)^{-2} & \text{if } b_0' \neq 0, \\ b_0+\dfrac{2\tau(\ln \varepsilon)^{-1}}{b_0 c_0'}+O(\ln \varepsilon)^{-2} & \text{if } b_0'=0, \end{cases} \tag{A.6}$$

$$c=\begin{cases} c_0-\dfrac{2\tau(\ln \varepsilon)^{-1}}{b_0 b_0'}+O(\ln \varepsilon)^{-2} & \text{if } b_0' \neq 0, \\ c_0-\dfrac{2\tau c_0(\ln \varepsilon)^{-1}}{b_0^2 c_0'}+O(\ln \varepsilon)^{-2} & \text{if } b_0'=0, \end{cases} \tag{A.7}$$

where

$$\varepsilon=-(\ln \mu)^{-1}$$

and $b_0(\tau)$ and $c_0(\tau)$ are defined by (A.3). Observe that the distance between this segment and the segment BC is of the order of $(\ln \varepsilon)^{-1}$. In particular,

$$b_M=4\left(1-\sqrt{\frac{2(p-n)}{\ln (1/\varepsilon)}}+O(\ln \varepsilon)^{-1}\right).$$

Segment EF.

$$c=\ln\left(b\sqrt{\frac{\varepsilon}{2}}\right)+2\nu\frac{(b-2)}{b}+8\frac{(4-b)}{b}+2b^{-1}\ln(2(b-2)^2)+O(\nu^{-1}) \tag{A.8}$$

with $b \in]2, 4[$ and ν defined by

$$(4-b)\exp(4(4-b))=2\varepsilon^{-1}(\nu+4)\exp((2-b)\nu).$$

In particular,

$$c_M=2\ln\frac{1}{\varepsilon}+7\ln 2-4+O(\ln \varepsilon)^{-1}.$$

Segment FG.

$$b=2+D(\alpha)+O(\varepsilon \ln \varepsilon)^2,$$

$$c=\tfrac{1}{2}(\ln 2\varepsilon+E(\alpha)+\varepsilon \ln \varepsilon+\alpha\varepsilon+O(\varepsilon \ln \varepsilon))^2$$

where $\alpha \in]-\infty, \infty[$ and $D(\alpha)$ and $E(\alpha)$ are defined by

$$D(\alpha)=\lim_{s\to\infty}\frac{du}{ds}, \qquad E(\alpha)=\lim_{s\to\infty}(D(\alpha)s-u),$$

$$\frac{d^2u}{ds^2}=\frac{\exp(-u)}{s}, \qquad \lim_{s\to 0}\frac{u}{s}-\ln(2s)=\alpha-d_n,$$

$$d_n=\sum_0^{n-1}\frac{(-1)^{k+1}}{n-k}.$$

In particular,

$$b_m = 2 + 1.822\varepsilon + \cdots .$$

Segment GH.

$$c = \frac{1}{2}\left(\ln\left(\frac{\varepsilon}{2}\right) + 2\ln b + \varepsilon\left(\frac{1}{b-2} + \ln\frac{b-2}{b} + d_n + .577\right) + O(\varepsilon^2)\right).$$

In particular,

$$c_m = \tfrac{1}{2}(\ln(2\varepsilon) + \sqrt{\varepsilon} + O(\varepsilon \ln \varepsilon)).$$

Observe that the asymptotics (A.2), (A.6) and (A.7) break down for sufficiently small values of τ; a refined analysis of the neighborhood of the point (b_c, c_c) would give the number of turns of the curve $b - c$ around the critical point (which, of course, is finite for any small, but fixed, value of μ and increases with μ^{-1}). Dotted lines in the case $n - p = -1$ correspond, in Fig. 8, to numerical computations of (A.1).

R. ARIS. *The Mathematical Theory of Diffusion and Reaction in Permeable Catalysts*, Vol. 1, Clarendon Press, Oxford, 1975.

J. J. CARBERRY AND J. HUTCHINGS, *The influence of surface coverage on catalytic effectiveness and selectivity: The isothermal and nonisothermal cases*, AIChE J., 12 (1966), pp. 20–23.

P. SCHNEIDER, P. MITSCHKA AND V. S. BESCOV, *Effect of internal diffusion on catalytic reactions, V: Nonisothermal case with a monomolecular Langmuir–Hinshelwood rate equation*, Colln Czech. Chm. Commun. Engl. Edn., 33 (1968), pp. 3598–3617.

T. G. SMITH, J. ZAHRADNIK AND J. J. CARBERRY, *Nonisothermal inter-intraphase effectiveness factors for negative order kinetics-CO oxidation over* Pt, Chem. Engrg. Sci., 30 (1975), pp. 763–767.

C. J. PEREIRA AND A. VARMA, *Uniqueness criteria of the steady state in automotive catalysis*, Chem. Engrg. Sci., 33 (1978), pp. 1645–1657.

J. L. URRUTIA AND A. LIÑÁN, *Steady heat and mass transfer in porous catalyst particles*, in Development of an Analytical Model of Hydrazine Decomposition Motors, Instituto Nacional de Técnica Aeroespacial, Stec Contract 1121/70 AA, Part III, Madrid, 1975.

A.K KAPILA AND B. J. MATKOWSKY, *Reactive-diffusive systems with Arrhenius kinetics: Multiple solutions, ignition and extinction*, this Journal, 36 (1979), pp. 373–389.

A. K. KAPILA, B. J. MATKOWSKY AND J. M. VEGA, *Reactive-diffusive systems with Arrhenius kinetics: Peculiarities of the spherical geometry*, this Journal, 38 (1980), pp. 382–401.

J. M. VEGA AND A. LIÑÁN, *Singular Langmuir–Hinshelwood reaction-diffusion problems: Strong adsorption under quasi-isothermal conditions*, this Journal, 42 (1982), pp. 1047–1068.

J. D. MURRAY, *A simple method for obtaining approximate solutions for a class of diffusion-kinetic enzyme problems, I: General class and illustrative examples*, Math. Biosci., 2 (1968), pp. 379–411.

V. R. ENDEM, *Gaskugeln, Anwendug der Mechanischem Warmentheorie auf Kosmologie*, B. G. Tuebner, Leipzig, 1907

D. D. JOSEPH AND T. S. LUNDGREN, *Quasilinear Dirichlet problems driven by positive sources*, Arch. Rational Mech. Anal., 49 (1973), pp. 241–269.

J. J. STEGGERDA, *Thermal stability: An extension of Frank-Kamenetsky's theory*, J. Chem. Phys., 43 (1965), pp. 4446–4448.

J. F. CLARKE, *Parameter perturbations in flame theory*, Progr. Aerospace Sci., 16 (1975), pp. 3–29.